

Plasmonic Terahertz Waveguide Based on Anisotropically Etched Silicon Substrate

Shanshan Li, Mohammad M. Jadidi, Thomas E. Murphy, *Senior Member, IEEE*, and Gagan Kumar

Abstract—We experimentally examine anisotropically etched silicon surfaces for terahertz (THz) plasmonic guided wave applications. Highly doped silicon surfaces are anisotropically etched to form a one-dimensional array of subwavelength concave pyramidal troughs. The plasmonic waveguides are found to support highly confined guided modes both in transverse and longitudinal directions. The resonant frequencies of the modes can be controlled by adjusting the geometrical parameters of the troughs. The existence of guided modes in plasmonic waveguides is also established through finite-element-based numerical simulations. These waveguides could provide a silicon-based alternative to metallic waveguides for use in future THz devices.

Index Terms—Anisotropic etching, plasmonics, subwavelength structures.

I. INTRODUCTION

IN RECENT YEARS, there has been significant interest in developing guided wave components operating in the terahertz (THz) regime for applications that include bio-sensing [1], imaging [2], slow light devices [3], modulators, and lasers [4]. Metal films have been a favorite candidate for THz waveguides because of their negligible dielectric and ohmic losses [5]–[7]. Numerous waveguide techniques have been proposed based upon planar thin metal films which include parallel-plate [8], [9], hollow cylindrical [10], and rectangular waveguides [11] and metal wire waveguides [12]. For many applications, the THz waveguide must provide confinement in both transverse and lateral directions.

Plasmonic waveguides, in which an electromagnetic wave is confined at the surface of a metallic or other negative index material, offer a simple geometry for waveguiding, and can provide subwavelength confinement of the guided mode [13], [14]. However, traditional plasmonic materials (including metals and doped semiconductors) are highly conductive at THz frequencies, which leads to a poorly confined plasmonic mode with

negligible penetration into the conductive substrate. By corrugating or periodically patterning the conductive surface, it is possible to construct a slow-light structure that mimics the plasmonic dispersion relation seen at optical wavelengths [15], [16]. These so-called ‘spoon’ or ‘designer’ plasmons have been extensively studied and demonstrated using corrugated metallic films at THz frequencies. These waveguides promise highly confined THz modes and centimeter-scale propagation length [17]–[22]. However, metallic structures are more challenging to fabricate, and are often incompatible with traditional semiconductor processes. There is a need for alternative solutions for semiconductor-based confined waveguides in the THz regime.

Intrinsic silicon has been a favorable substrate for fabricating metamaterials and other devices at THz frequencies because of the negligible absorption loss associated with it [23]–[25]. However, the potential of silicon substrates for THz plasmonic waveguide applications has yet to be established. Silicon, when heavily doped, can exhibit metallic properties [26], [27] and therefore has potential to replace metal for THz waveguide applications. Furthermore, the dielectric properties of silicon can potentially be tailored by controlling the carrier concentration through doping, implantation, optical illumination, or electrical injection—a degree of freedom that is absent in most metals [24]. Compatibility with existing semiconductor fabrication techniques makes silicon an attractive candidate material for THz devices.

Recently, silicon V-groove corrugations were shown to provide vertical confinement of THz waves to a surface [26], [28]. Here, we show that a one-dimensional array of finite-width silicon troughs can serve as a THz plasmonic waveguide, providing confinement in both transverse directions. Heavily doped crystalline silicon is anisotropically etched to produce a periodic array of rectangular pyramidal troughs [29], which confine and guide the THz signal. Numerous waveguide structures, with different geometrical parameters, are fabricated and measured, and the observed mode behavior is validated through finite-element-method-based electromagnetic numerical simulations (CST Microwave Studio). Based upon our experimental waveguide observations, we consider an aperiodic structure in which a resonant defect is introduced in an otherwise periodic array. We show that, in such a structure, the THz wave can be longitudinally localized in a single trough of the waveguide.

II. FABRICATION AND MEASUREMENT

Fig. 1 illustrates the geometry of the silicon waveguide structures considered here, along with a top-down micrograph showing a completed structure. The waveguide samples were fabricated from (001) oriented boron-doped silicon substrates ($\rho = 2\text{--}5\text{ m}\Omega\text{cm}$). A $1.3\text{-}\mu\text{m}$ -thick oxide layer was deposited

Manuscript received January 31, 2014; revised March 22, 2014; accepted May 13, 2014. Date of publication June 10, 2014; date of current version June 26, 2014.

S. Li and M. M. Jadidi are with the Department of Electrical and Computer Engineering University of Maryland, College Park, MD 20742 USA (e-mail: lishanshan228@gmail.com).

T. E. Murphy is with the Department of Electrical and Computer Engineering and the Institute for Research in Electronics and Applied Physics, University of Maryland, College Park, MD 20742 USA.

G. Kumar was with the Institute for Research in Electronics and Applied Physics, University of Maryland, College Park, MD 20742 USA. He is currently with the Department of Physics, Indian Institute of Technology Guwahati, Guwahati 781039, India (e-mail: gk@iitg.ernet.in).

Color versions of one or more of the figures in this paper are available online at <http://ieeexplore.ieee.org>.

Digital Object Identifier 10.1109/TTHZ.2014.2325739

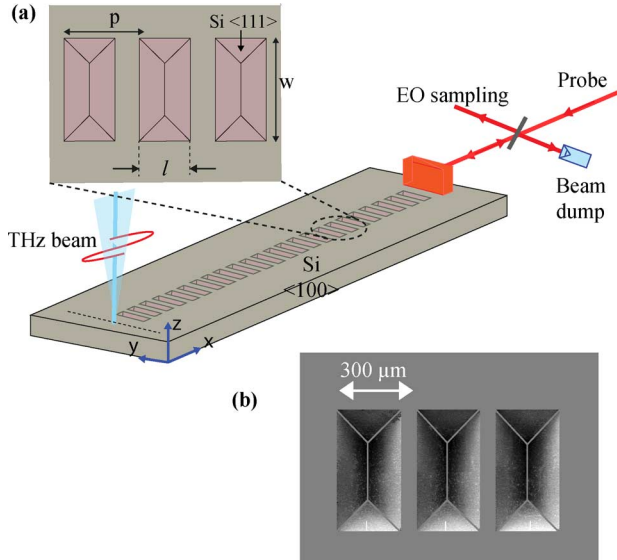


Fig. 1. (a) Schematic of the plasmonic waveguide comprising a periodic array of pyramidal troughs in silicon. A rectangular groove at the input end is used to promote coupling in the out-of-plane direction. (b) Scanning electron micrograph of a portion of anisotropically etched troughs in silicon.

using chemical vapor deposition and patterned using contact photolithography and reactive ion etching to form rectangular windows that define the regions to be etched. The silicon was next etched in a mixture of potassium hydroxide, water, and isopropanol in the ratio of 60:30:10. The etching was conducted at a temperature of 80 °C with approximately 0.4- $\mu\text{m}/\text{s}$ etching rate. The anisotropic etching forms a concave rectangular trough bounded by four facets aligned with the (111), ($\bar{1}\bar{1}1$), ($\bar{1}1\bar{1}$), and ($1\bar{1}\bar{1}$) crystal planes, as shown in Fig. 1(b). Each side facet is inclined at an angle of 54.73° with respect to the (001) surface. After fabrication, the remaining oxide was removed using a buffered oxide etch (BOE). It should be mentioned that, while the orientation of the pyramidal troughs is constrained by crystallographic planes, the placement and size of these features can be lithographically controlled. While a linear array of features (as considered here) is the most straightforward configuration, more complex geometries can also be imagined, such as a staircase array to allow for slanted or curved topologies [30].

Fig. 1 shows the modified THz time-domain spectroscopy system that was employed to characterize the plasmonic waveguides [30]. An optical beam at 800 nm wavelength with pulse duration 43 fs having average power of 1.2 W at 1 kHz is used to generate a THz pulse through a LiNbO₃ crystal via optical rectification. The *S*-polarized pump beam incident on the nonlinear crystal generates broadband THz radiation which is collected and collimated using off-axis parabolic mirrors. The focused THz beam of about 3 mm diameter is normally incident on the coupling groove that is 2.5 mm long and 300 μm in width. The incident THz wave is polarized in the *x*-direction (i.e., parallel to the direction of the waveguide), in order to allow for coupling into the plasmonic mode. A 300- μm -long \times 100- μm -deep coupling groove is separately fabricated using deep reactive ion etching (DRIE) near the input side of the waveguide to facilitate scattering of the normally incident THz wave into the surface plasmonic mode. By comparing the intensity measured

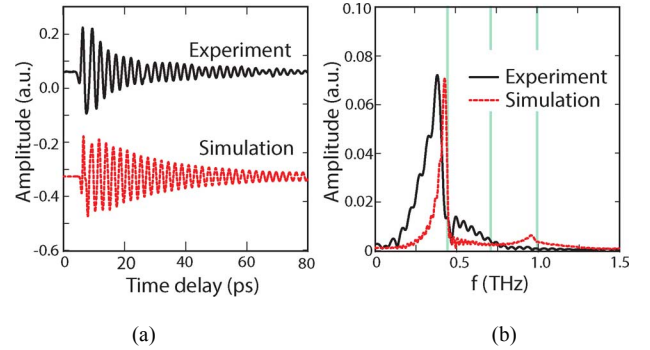


Fig. 2. (a) Time-domain signal and (b) corresponding frequency-domain spectra of the transmitted THz waveform for a 300- μm period array of 500 \times 250 μm (*w* \times *l*) troughs.

after the coupling groove with that obtained by replacing the device with an off-axis parabolic mirror, we estimated input coupling efficiency to be 10%. After propagating along the patterned surface, the emerging THz wave is measured using a ZnTe crystal of thickness 1 mm, brought into close proximity to the surface. A probe beam passes through the ZnTe crystal, and is detected using a polarization beamsplitter and balanced detector, thereby sampling the THz waveform. The probe beam, which is co-linear with the waveguide, is focused through the ZnTe crystal with a beam waist of 0.3–0.4 mm and pulse energy of 1 μJ . The probe beam is positioned approximately 0.5 mm above the pillar surface, thereby ensuring that there is no interaction with the substrate.

III. RESULTS AND DISCUSSION

In our study, we fabricated three waveguide samples, each with a length of 5 cm and periodicity of $p = 300 \mu\text{m}$. The length and width of the rectangular troughs were varied. Fig. 2 shows both the experimentally observed (black) and numerically simulated (red) time domain signals for the case where the trough dimensions were 500 \times 250 μm (*w* \times *l*). The corresponding frequency-domain spectra, obtained by Fourier transform, are shown in Fig. 2(b). The simulations were conducted using the finite-element time-domain method, with perfect electrical conducting boundary conditions assumed at the silicon surface. For the dopant concentration considered here, the Drude model predicts a relative permittivity of $\epsilon = (-1.3 + 2.0i) \times 10^4$ at 1 THz, which is sufficiently large to justify treatment as a perfect conductor. To confirm the validity of the assumed PEC boundary conditions, we have repeated selected simulations using a more accurate 3-D Drude model, and an equivalent surface impedance model, and found no significant difference in the numerical results.

Both experiment and simulation exhibit resonant behavior, as evidenced by the long-lived oscillations in the time-domain traces and the corresponding null in the frequency spectra at 0.45 THz. The observed resonant frequency agrees well with that predicted numerically. Some discrepancies between the experimental measurement and numerical prediction exist, which we attribute to diffractive losses, interference from unguided radiation, and multiple internal reflections in the ZnTe detection crystal—effects that are not captured by the simulation.

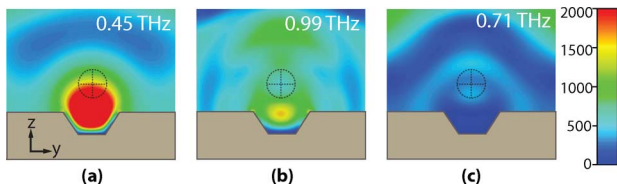


Fig. 3. Simulated electric field profile evaluated at the center of a trough (a) at the resonant frequency (0.45 THz), (b) higher order resonance (0.99 THz), and (c) off-resonance (0.71 THz). The dashed cross hairs indicate the approximate size and position of the optical probe beam used in the experiment.

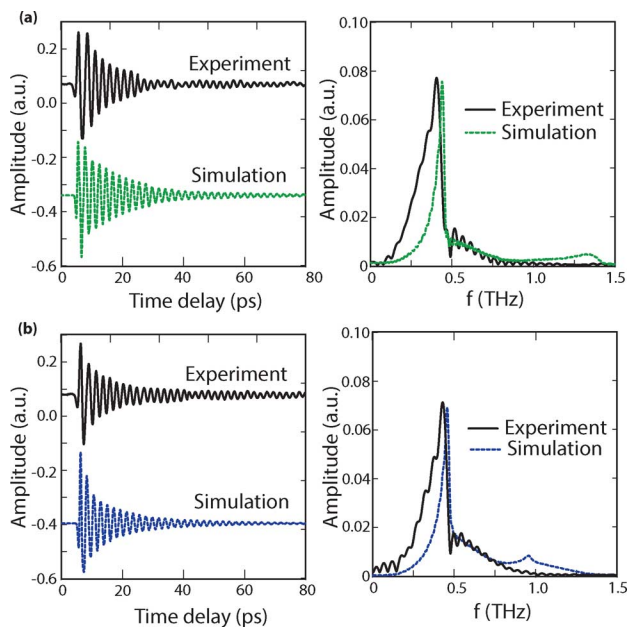


Fig. 4. (a) Experimentally observed and simulated time-domain signal and (b) corresponding frequency-domain spectra for an array of troughs with dimensions (a) $500 \times 200 \mu\text{m}$ and (b) $400 \times 250 \mu\text{m}$. In all cases the period was $p = 300 \mu\text{m}$.

In order to better illustrate the mode behavior, in Fig. 3, we plot the numerically simulated electric field at the resonant frequency, evaluated in a cross-sectional plane at the center of one trough. Clearly, at the resonant frequency of 0.45 THz, the field is highly confined within the trough. The simulated traces also show evidence of a higher order resonance 0.99 THz that is not as tightly confined, as shown in Fig. 3(b). By contrast, at the off-resonance frequency of 0.71 THz, the field profile is not confined to the surface, as shown in Fig. 3(c). Because of losses at higher frequencies, the higher order resonances were more difficult to observe in the experimentally measured spectra.

Fig. 4(a) shows similar measurements and simulations performed on devices with trough dimensions of $500 \times 200 \mu\text{m}$ and $400 \times 250 \mu\text{m}$ ($w \times l$). While the overall responses are similar, the resonant frequencies for the fundamental mode show a slight red-shift (0.47 THz and 0.48 THz, respectively) in comparison to the that seen in Fig. 2, which is well confirmed by the numerical simulations.

In Fig. 5, we show the dispersion relations calculated numerically using a finite-element eigenmode solver for the three waveguides examined experimentally in Figs. 2–4. The dispersion relation was calculated by numerically modeling one unit cell of the periodic structure, using Bloch boundary conditions

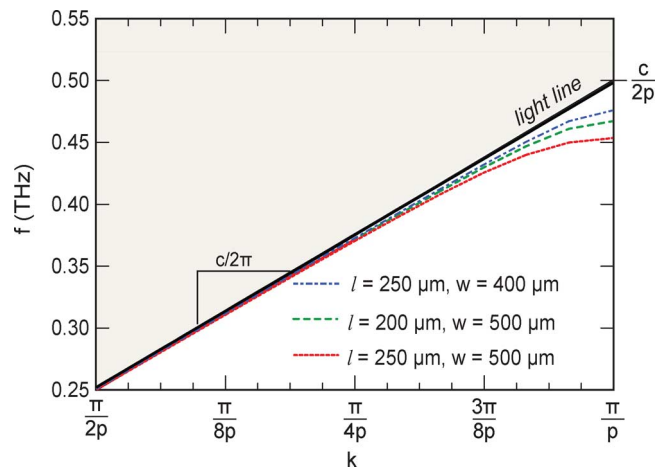


Fig. 5. Numerically computed dispersion relation of the fundamental modes, calculated over the first Brillouin zone, for three different geometrical parameters.

along the direction of propagation and absorbing boundary conditions in the transverse directions. Perfect electrical conducting boundary conditions were assumed at the silicon surface, as approximated for heavily doped silicon. The black solid line in the figure corresponds to the light line for plane waves propagating in vacuum. The blue, green and red curves correspond to surface electromagnetic modes supported by the periodically patterned troughs with dimensions $(w \times l) = 400 \times 250$, 500×200 , and $500 \times 250 \mu\text{m}$, respectively. The periodicity in all of the cases was held constant at $p = 300 \mu\text{m}$. Within the first Brillouin zone, the wavenumber and frequency increase monotonically, but with a reduced group and phase velocity compared with vacuum waves. The group velocity reduces to zero at the first Brillouin zone boundary ($k_x = \pi/p$), corresponding to the excitation of a confined resonant surface mode. The calculated frequency of the first Brillouin zone edge is observed to match the null-frequency seen in experiments and simulations. One can obtain the group velocity of the surface modes from the slope of the dispersion relations depicted in Fig. 5. The group velocity decreases with increasing depth of the trough, and approaches zero at the first Brillouin boundary.

In order to examine the dependence of the resonant frequency on the dimensions of the troughs, we carried out simulations for the various combinations of length, width, and periodicity. The results are shown through a color and contour plot in Fig. 6. The length and width are plotted on the horizontal and vertical directions respectively, normalized relative to the period p . The resonant frequency, normalized to $c/2p$, is shown by the contours and color map. In the limit that the length of the trough is small compared with the period, the resonant frequency approaches $c/2p$ indicating that even near the Brillouin edge there is no substantial deviation from the vacuum light line. In the case when width is very large, the resonant frequency approaches a constant value characteristic of what is expected for infinitely long (1-D) V-grooves [26]. In order to quantify the propagation loss of the waveguide, we numerically calculated the frequency-dependent attenuation coefficient for one of the experimentally examined waveguide. The results for the waveguide with parameters $(w \times l) = 500 \times 250 \mu\text{m}$ and $p = 300 \mu\text{m}$ are shown in Fig. 7. One may note that the propagation length

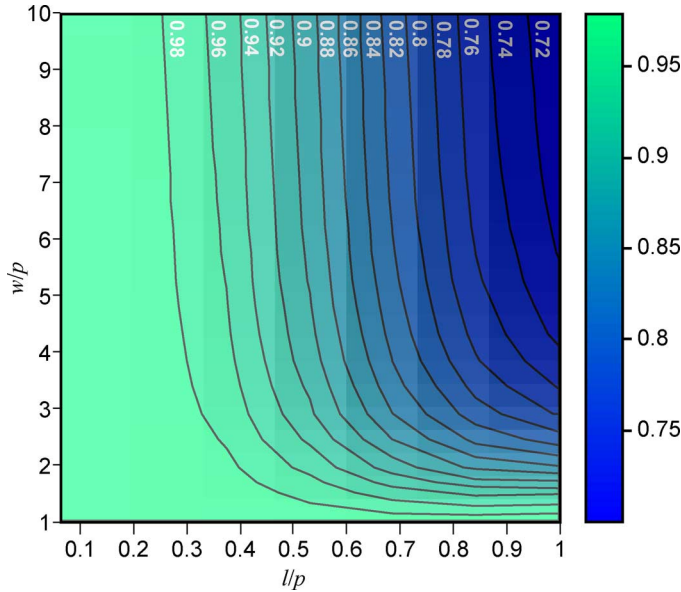


Fig. 6. Contour plot of calculated resonant frequency (normalized to $c/2p$) as a function of the dimensions of the pyramidal trough.

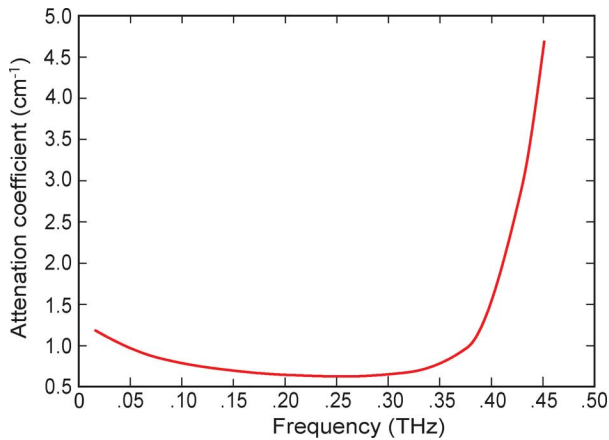


Fig. 7. Waveguide attenuation coefficient versus frequency for the parameters for the $(w \times l) = 500 \times 250 \mu\text{m}$ and $p = 300 \mu\text{m}$.

is higher the around resonant frequency. The loss is higher on both sides of the resonance. On the higher frequency side of the resonance, i.e., after the null frequency, attenuation loss rises significantly as expected.

The plasmonic confinement in corrugated waveguide structures is a resonant effect with a frequency that depends on the size and shape of the pyramidal troughs. Many THz applications could benefit from further confinement in the longitudinal direction. We numerically investigated this possibility by simulating a periodic array with one dissimilar defect introduced at the center, as shown in Fig. 8. In this simulation, the defect trough has dimensions of $(w \times l) = 500 \times 250 \mu\text{m}$. The experimental and simulated results presented in Fig. 2 suggest that these dimensions should exhibit a resonant frequency near 0.45 THz. The surrounding troughs measured $500 \times 50 \mu\text{m}$ and formed a shallow, linear array of 6 mm length on either side of the defect. Fig. 8 plots the transverse electric field evaluated at the silicon surface, calculated at 0.45 THz (blue) and at the off-resonant

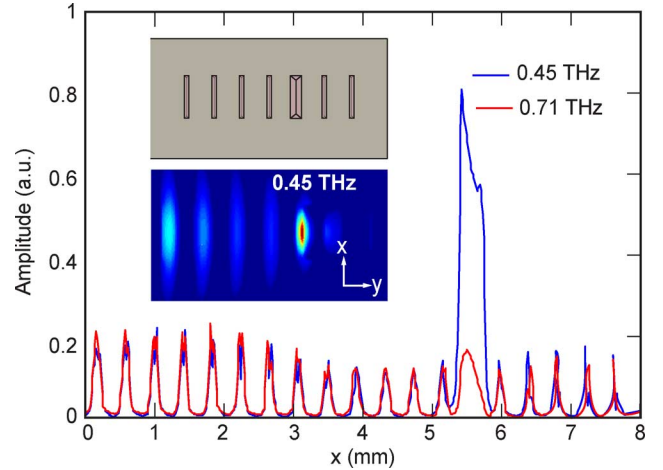


Fig. 8. Simulated electric field amplitude for a periodic structure with a defect at the center, showing evidence of longitudinal confinement. The amplitudes are shown at the predicted resonant frequency of 0.45 THz (blue) and at the off-resonant frequency of 0.71 THz (red).

frequency of 0.71 THz (red). As expected, when excited near the resonant frequency (0.45 THz), the plasmonic field shows significant enhancement in the defect, indicating that longitudinal confinement is possible by spatially tailoring the device dimensions. The inset to Fig. 8 plots the electric field profile calculated on resonance, further confirming the spatial localization of the resonant mode. It is important to mention that deeper structure can result in further confinement of the modes, however in the case examined here, depth is limited by the angle dependent etching. Therefore one needs to explore techniques of achieving waveguide structures with higher aspect ratio (depth to width ratio) in semiconductors.

IV. CONCLUSION

We have designed, simulated, fabricated, and characterized THz plasmonic waveguides that exhibit highly confined guided mode propagation along the patterned structures. The plasmonic waveguides comprising pyramidal troughs are fabricated using anisotropic etching of doped crystalline silicon. The resonant frequencies associated with confined modes are shown to depend on the dimensions of the pyramidal troughs and hence can be tailored by appropriate design. In general, we observe a red-shift in the resonant frequency as the troughs are made deeper, corresponding to tighter confinement in the structure. The experimental observations are confirmed using finite element simulations. Further, we numerically confirm the possibility of producing a fully localized mode by introducing a defect in an otherwise periodic array. The ability to achieve plasmonic confinement and localization in an all-silicon material system could have important applications for future THz components and sensors.

REFERENCES

- [1] J. S. Melinger, N. Laman, S. S. Harsha, and D. Grischkowsky, "Line narrowing of terahertz vibrational modes for organic thin polycrystalline films within a parallel plate waveguide," *Appl. Phys. Lett.*, vol. 89, no. 25, 2006, Art. ID 251110.

- [2] M. M. Awad and R. A. Cheville, "Transmission terahertz waveguide-based imaging below the diffraction limit," *Appl. Phys. Lett.*, vol. 86, no. 22, 2005, Art. ID 221107.
- [3] Q. Gan, Z. Fu, Y. J. Ding, and F. J. Bartoli, "Ultrawide-bandwidth slow-light system based on THz plasmonic graded metallic grating structures," *Phys. Rev. Lett.*, vol. 100, Jun. 2008, Art. ID 256803.
- [4] H.-T. Chen, W. J. Padilla, J. M. O. Zide, A. C. Gossard, A. J. Taylor, and R. D. Averitt, "Active terahertz metamaterial devices," *Nature*, vol. 444, pp. 597–600, 2006.
- [5] R. Mendis and D. Grischkowsky, "Undistorted guided-wave propagation of subpicosecond terahertz pulses," *Opt. Lett.*, vol. 26, no. 11, pp. 846–848, Jun. 2001.
- [6] G. Gallot, S. P. Jamison, R. W. McGowan, and D. Grischkowsky, "Terahertz waveguides," *J. Opt. Soc. Amer. B*, vol. 17, no. 5, pp. 851–863, May 2000.
- [7] A. Rusina, M. Durach, K. A. Nelson, and M. I. Stockman, "Nanoconcentration of terahertz radiation in plasmonic waveguides," *Opt. Express*, vol. 16, no. 23, pp. 18576–18589, Nov. 2008.
- [8] S. Coleman and D. Grischkowsky, "Parallel plate THz transmitter," *Appl. Phys. Lett.*, vol. 84, no. 5, pp. 654–656, 2004.
- [9] J. Liu, R. Mendis, and D. M. Mittleman, "The transition from a TEM-like mode to a plasmonic mode in parallel-plate waveguides," *Appl. Phys. Lett.*, vol. 98, no. 23, 2011, Art. ID 231113.
- [10] O. Mitrofanov and J. A. Harrington, "Dielectric-lined cylindrical metallic THz waveguides: Mode structure and dispersion," *Opt. Express*, vol. 18, no. 3, pp. 1898–1903, Feb. 2010.
- [11] F. Kong, B.-I. Wu, H. Chen, and J. A. Kong, "Surface plasmon mode analysis of nanoscale metallic rectangular waveguide," *Opt. Express*, vol. 15, no. 19, pp. 12331–12337, Sep. 2007.
- [12] K. Wang and D. M. Mittleman, "Metal wires for terahertz wave guiding," *Nature*, pp. 376–379, 2004.
- [13] F. J. Garcia-Vidal, L. Martin-Moreno, and J. B. Pendry, "Surfaces with holes in them: New plasmonic metamaterials," *J. Opt. A, Pure Appl. Opt.*, vol. 7, no. 2, p. S97, 2005.
- [14] D. Gacemi, J. Mangeney, R. Colombelli, and A. Degiron, "Subwavelength metallic waveguides as a tool for extreme confinement of THz surface waves," *Sci. Rep.*, vol. 3, p. 1369, 2013.
- [15] J. B. Pendry, L. Martin-Moreno, and F. J. Garcia-Vidal, "Mimicking surface plasmons with structured surfaces," *Science*, vol. 305, no. 5685, pp. 847–848, 2004.
- [16] R. E. Collin, *Field Theory of Guided Waves*, 2nd ed. New York, NY, USA: Wiley/IEEE, 1990.
- [17] A. I. Fernández-Domínguez, L. Martin-Moreno, F. J. Garcia-Vidal, S. R. Andrews, and S. A. Maier, "Spoof surface plasmon polariton modes propagating along periodically corrugated wires," *IEEE J. Sel. Topics Quantum Electron.*, vol. 14, no. 6, pp. 1515–1521, Nov./Dec. 2008.
- [18] C. R. Williams, S. R. Andrews, S. A. Maier, A. I. Fernández-Domínguez, L. Martin-Moreno, and F. J. Garcia-Vidal, "Highly confined guiding of terahertz surface plasmon polaritons on structured metal surfaces," *Nat. Photon.*, vol. 2, pp. 175–179, 2008.
- [19] G. Kumar, S. Pandey, A. Cui, and A. Nahata, "Planar plasmonic terahertz waveguides based on periodically corrugated metal films," *New J. Phys.*, vol. 13, no. 3, 2011, Art. ID 033024.
- [20] W. Zhu, A. Agrawal, A. Cui, G. Kumar, and A. Nahata, "Engineering the propagation properties of planar plasmonic terahertz waveguides," *IEEE J. Sel. Topics Quantum Electron.*, vol. 17, no. 1, pp. 146–153, Jan./Feb. 2011.
- [21] T. Jiang, L. Shen, J.-J. Wu, T.-J. Yang, Z. Ruan, and L. Ran, "Realization of tightly confined channel plasmon polaritons at low frequencies," *Appl. Phys. Lett.*, vol. 99, no. 26, 2011, Art. ID 261103.
- [22] A. I. Fernández-Domínguez, E. Moreno, L. Martín-Moreno, and F. J. Garcia-Vidal, "Guiding terahertz waves along subwavelength channels," *Phys. Rev. B*, vol. 79, Jun. 2009, Art. ID 233104.
- [23] H. Tao, A. C. Strikwerda, M. Liu, J. P. Mondia, E. Ekmekci, K. Fan, D. L. Kaplan, W. J. Padilla, X. Zhang, R. D. Averitt, and F. G. Omenetto, "Performance enhancement of terahertz metamaterials on ultrathin substrates for sensing applications," *Appl. Phys. Lett.*, vol. 97, no. 26, 2010, Art. ID 261909.
- [24] D. R. Chowdhury, R. Singh, J. F. O'Hara, H.-T. Chen, A. J. Taylor, and A. K. Azad, "Dynamically reconfigurable terahertz metamaterial through photo-doped semiconductor," *Appl. Phys. Lett.*, vol. 99, Dec. 2011, Art. ID 231101.
- [25] J. Gu, R. Singh, A. K. Azad, J. Han, A. J. Taylor, J. F. O'Hara, and W. Zhang, "An active hybrid plasmonic metamaterial," *Opt. Mater. Exp.*, vol. 2, no. 1, pp. 31–37, Jan. 2012.
- [26] S. Li, M. M. Jadidi, T. E. Murphy, and G. Kumar, "Terahertz surface plasmon polaritons on a semiconductor surface structured with periodic V-grooves," *Opt. Exp.*, vol. 21, no. 6, pp. 7041–7049, Mar. 2013.
- [27] H. Seidel, L. Csepregi, A. Heuberger, and H. Baumgartel, "Anisotropic etching of crystalline silicon in alkaline solutions," *J. Electrochem. Soc.*, vol. 137, no. 11, pp. 3612–3626, 1990.
- [28] J. J. Wood, L. A. Tomlinson, O. Hess, S. A. Maier, and A. I. Fernández-Domínguez, "Spoof plasmon polaritons in slanted geometries," *Phys. Rev. B*, vol. 85, Feb. 2012, Art. ID 075441.
- [29] S. Sriram and E. P. Supertzi, "Novel V-groove structures on silicon," *Appl. Opt.*, vol. 24, no. 12, pp. 1784–1787, Jun. 1985.
- [30] G. Kumar, S. Li, M. M. Jadidi, and T. E. Murphy, "Terahertz surface plasmon waveguide based on a 1-D array of silicon pillars," *New J. Phys.*, vol. 15, 2013, Art. ID 085031.



Shanshan Li received the B.Eng. degree in electrical and electronic engineering from the University of Science and Technology of China, Hefei, China, in 2010. She is currently working toward the Ph.D. degree in electrical and computer engineering at the University of Maryland, College Park, MD, USA.

Her research interests include terahertz nonlinear optics and terahertz devices.



Mohammad M. Jadidi received the B.S. degrees in electrical engineering and physics from Sharif University of Technology, Tehran, Iran, in 2011.

Since 2012, he has been a Graduate Research Assistant with the Photonics Research Laboratory, University of Maryland, College Park, MD, USA.



Thomas E. Murphy (M'94–SM'07) received the B.S. degrees in electrical engineering and physics from Rice University, Houston, TX, USA, in 1994, and the M.S. and Ph.D. degrees in electrical and computer engineering from the Massachusetts Institute of Technology, Cambridge, MA, USA, in 1997 and 2001, respectively.

He was a Member of the Technical Staff at MIT Lincoln Laboratory from 2001 to 2002 and joined the faculty at the University of Maryland, College Park, MD, USA, in 2002. He holds a joint appointment as

a Professor with the Department of Electrical and Computer Engineering and Director of the Institute for Research in Electronics and Applied Physics.



Gagan Kumar received the M.S. degree from Kurukshetra University, Kurukshetra, India, in 2003, and the Ph.D. degree from the Indian Institute of Technology Delhi, New Delhi, India, in 2008.

He is currently an Assistant Professor with the Indian Institute of Technology Guwahati (IIT G), Guwahati, India. Prior to joining at IIT G in 2013, he was a Postdoctoral Research Associate with the Institute for Research in Electronics and Applied Physics, University of Maryland, College Park, MD, USA. He was also a Postdoctoral Researcher with

the Department of Electrical and Computer Engineering, University of Utah, Salt Lake City, UT, USA, from 2008 to 2010. His research focus primarily has been in investigating and building terahertz plasmonic devices using thin metal films and doped silicon surfaces.